PHYSICAL REVIEW B **77**, 041401(R) (2008)

Ultrafast photoinduced changes of eigenfunctions of localized plasmon modes in gold nanorods

Kohei Imura and Hiromi Okamoto*
Institute for Molecular Science and The Graduate University for Advanced Studies, Okazaki 444-8585, Japan
(Received 1 November 2007; published 2 January 2008)

Ultrafast transient responses in single gold nanorods are visualized in real space by femtosecond pump-probe measurements using a near-field optical microscope. The observed transient images show characteristic features, and the features are strongly dependent on the size of the rod. It is revealed that the features arise from changes in the plasmon-mode wave function upon elevation of the electronic temperature of the nanorod induced by photoexcitation.

DOI: 10.1103/PhysRevB.77.041401 PACS number(s): 78.67.Bf, 78.47.−p, 87.64.mt

The electronic and optical properties of nanoparticles and their assemblies, as well as nonlinear and ultrafast characteristics, are significantly different from bulk materials. Such unique properties of nanomaterials are essential for the development of novel material functions and are closely correlated to ultrafast electron dynamics. For a thorough understanding of electron dynamics, spatially resolved ultrafast measurements, in particular those capable of resolving positions on a single nanoparticle, may provide essential information that can never be accessed by other means. This information is hardly available using conventional far-field microscopes because of the diffraction limit of light, whereas recently developed near-field methodologies are feasible for that.[1,2] Basic experimental attempts at near-field ultrafast studies have been recently reported for the electronic excitation of metal nanoparticles.[3]

The collective excitation of free electrons in metal nanoparticles, known as localized surface plasmon (LSP) resonances,[4–6] is one of the important elementary excitations that determine the electronic properties of nanoparticles. The studies of LSP in noble-metal nanoparticles have expanded their influence recently from various surface-enhanced spectroscopies[7–9] to novel nanometric optical devices and waveguides.[6,10] The potentialities of LSPs arise from their capacity for effective confinement and enhancement of electromagnetic fields in nanometric space in the vicinity of nanoparticles.[11,12]

The studies of LSPs are not limited to spherical particles, but have extended to nanoparticles of various shapes such as nanorods because of a unique feature in which optical properties are tunable by changing the structure parameters (e.g., aspect ratio).[13,14] Far-field optical measurements for single gold nanorods enabled a discussion on shape-dependent spectroscopic properties.[15,16] Nonlinear and ultrafast measurements for single noble-metal nanoparticles were also performed, and information on electron dynamics was obtained.[17,18] To understand the shape-dependent dynamics of LSPs in the nanoparticle, however, visualization of dynamic behavior of the LSP modes of the single particle and simultaneous observation of the particle shape are indispensable. This is achievable through spatially resolved near-field ultrafast imaging of single nanoparticles, as mentioned previously. In the present study, we succeeded in near-field ultrafast imaging of LSPs in single gold nanorods based on a previously reported method[3] and the physical origin of the images we obtained are revealed. The present results may not only bring a new dimension to studies on plasmon resonances, but also serve as a basis for a new scheme of coherent control of elementary excitations.

We used chemically synthesized single gold nanorods (diameters 15–40 nm) (Ref. 19) dispersed on a cover slip as the sample. An apertured-type near-field optical microscope was operated under ambient conditions.[2] The lateral spatial resolution of the near-field measurement was ca. 50 nm. The distance between the sample surface and the probe tip was regulated by the shear-force feedback method. A Xe discharge arc lamp was used as a light source for near-field transmission spectral and imaging measurements. For ultrafast near-field measurements, we used a mode-locked Ti:sapphire laser (λ =780 nm, <100 fs, 80 MHz). The time resolution was ca. 100 fs at the probe tip. To visualize the ultrafast transient image of the nanorod, we adopted an equal-pulse pump and probe transient transmission scheme in the near field. The average incident power on the rod was less than 3 μW. Under these conditions, the gold nanorod was stable at least 12 h without any topographical or spectroscopic degradation.

First, we analyzed static near-field optical features (images and spectra) of nanorods. A typical topographic image of a single gold nanorod (diameter 30 nm, length 300 nm: aspect ratio=10) is shown in Fig. 1(a). Transmission images were obtained by detecting photons polarized parallel to the long axis of the nanorod to observe the longitudinal LSP modes [Figs. 1(b) and 1(c)]. A dark oval-ring-like feature in Fig. 1(b), which corresponds to the outer rim of the topographic image in Fig. 1(a), is a "topographic artifact" and is of no physical interest. From the true optical feature in Fig. 1(b) consisting of two dark spots, it is evident that the excitation probability of the LSP depends on the position on the nanorod and oscillates along the long rod axis. On the other hand, in Fig. 1(c), the image shows one extinction maximum at the central part. These features are observed because of the high spatial resolution of spectral imaging and arise from the wave functions of resonant LSP modes.

Figures 2(a) and 2(b) show near-field transmission spectra polarized along the rod axis obtained at two points in the nanorod. The spectrum obtained at the end part of the nanorod [Fig. 2(a)] shows two longitudinal LSP resonance peaks near 620 nm and 750 nm, while the central portion [Fig. 2(b)] shows only one LSP peak near 620 nm. The position-dependent spectral features observed reflect spatial characteristics of the longitudinal LSP modes. The LSP mode with the resonance wavelength at 750 nm has a node at the center of

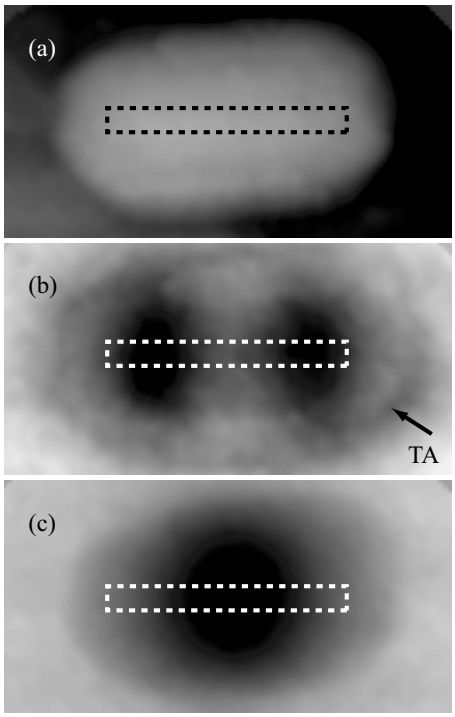

FIG. 1. (a) Topography of a single gold nanorod (diameter 30±5 nm×length300±50 nm). (b) and (c) Transmission images obtained at wavelengths of ca. 750 and 900 nm, respectively. A dotted square in each panel indicates an approximate shape of the nanorod estimated from (a). Note that "TA" in (b) indicates a topographic artifact (see the text). Transmission $[-(I-I_0)/I_0]$ ranges roughly from 0.0 (white) to 0.6 (black), where I and I_0 are intensities measured on the particle and at the bare substrate, respectively.

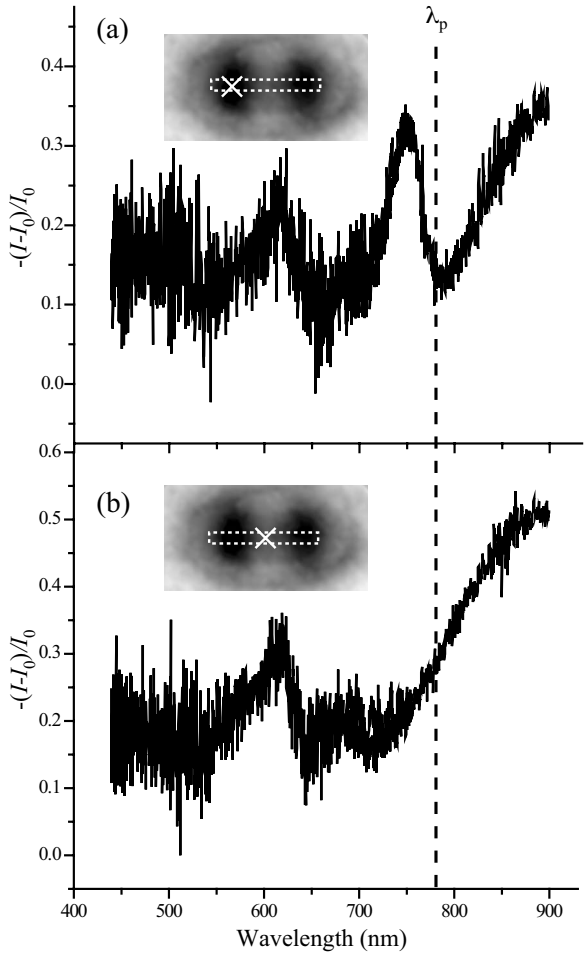

FIG. 2. Near-field transmission spectra obtained (a) at the end part and (b) at the central part of the nanorod. λ_p (=780 nm) indicates the wavelength used for the transient transmission measurements.

the rod [Fig. 1(b)], whereas resonance at the 620 nm has an antinode at the center. In addition to these resonance spectral peaks, we find a steep increase in extinction at the longer wavelength. This feature is ascribed to a blue-side wing of the fundamental dipolar LSP mode [Fig. 1(c)], whose resonance frequency is far beyond the measured spectral range.

Now, we present the near-field transient transmission image of the same single gold nanorod. In the near-field transient imaging, we adopted a pump-probe method. Photoexcitation by the pump pulse initiates a dynamic process and the probe pulse measures the following transmission change in the nanorod. Figure 3(a) shows a transient transmission image of the single gold nanorod observed at a pump-probe delay time of 600 fs. The bright and dark parts indicate the bleached and induced absorption regions, respectively. The image was obtained at an excitation wavelength of ~780 nm, where both the fundamental dipolar plasmon mode ($\lambda_{LSP}>1$ μm) and the second mode ($\lambda_{LSP}=750$ nm) can be excited. Notably, both the induced and bleached absorptions are observed at the same time in the single nanorod. It should be noted that dephasing of the plasmons in the gold nanorod is significant only at a very short delay time (up to ca. 20 fs),[15] and thus, the effect of mode selectivity is of minimal relevance to the transient image.

To elucidate the physical origin of the characteristic feature of the transient image, we simulated transient transmission images based on the theoretical calculation of the electromagnetic local density of states (LDOS). It has been shown that steady-state near-field transmission images of metal nanoparticles are well reproduced by the electromagnetic LDOS.[14,20] We assumed that the transient transmission change arises from variations in the LDOS upon photoexcitation, due primarily to the elevation of electronic temperature in the nanorod. Additionally, we assumed that electronic temperature increases is homogeneous in the rod at 600 fs after photoexcitation. Ultrafast measurements of thin (up to ~300 nm) gold films showed that the heat transport velocity in the direction normal to the surface is $\sim 10^8$ cm/s.[21] If electronic heat transport in the nanorods is as fast as that in the thin films, the electronic temperature in the 300-nm-length rod would be nearly homogeneous within 600 fs.

Following the Green dyadic formalism, the steady-state LDOS ρ is given by[20]

$$\rho(\vec{r},\omega,T) = -\frac{1}{\pi}\,\mathrm{Tr}[\mathrm{Im}\{\overleftrightarrow{G}(\vec{r},\vec{r},\omega,\varepsilon(T))\}], \qquad (1)$$

where, $\overleftrightarrow{G}$, $\vec{r}$, and ω denote, respectively, the Green dyadic of interest, position, and optical angular frequency and $\varepsilon(T)$ is

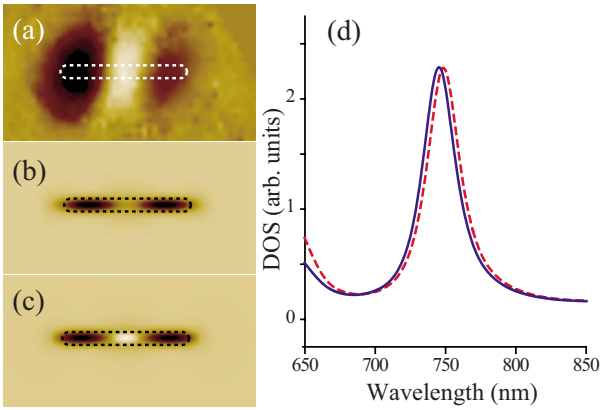

FIG. 3. (Color online) (a) Transient transmission image of a single gold nanorod observed at 600 fs delay time. A dotted square indicates an approximate shape (diameter 30 nm × length 300 nm) of the nanorod estimated from the topography measurement. Bright and dark parts indicate regions giving bleached and induced absorption, respectively. (b) and (c) Simulated transient transmission (LDOS change) images at 780 nm (b) and 920 nm (c) for the nanorod. Dark and bright parts indicate regions giving enhanced and reduced LDOS, respectively. (d) Calculated DOS spectra of the nanorod at room temperature (T_{elec}=300 K, solid curve) and at the elevated temperature ($T_{\mathrm{elec}}+\Delta T_{\mathrm{elec}}$=600 K, dashed curve).

the dielectric constant of the material at electronic temperature T. Since we presumed that the transient transmission change ($\Delta I_{\mathrm{transient}}$) at each position arises from variation in the LDOS due to the elevation of temperature, $\Delta I_{\mathrm{transient}}$ is given by the following equation:

$$\Delta I_{\mathrm{transient}}(\vec{r},\omega,T_{\mathrm{elec}},\Delta T_{\mathrm{elec}}) \propto \rho(\vec{r},\omega,T_{\mathrm{elec}}+\Delta T_{\mathrm{elec}})-\rho(\vec{r},\omega,T_{\mathrm{elec}}), \quad (2)$$

where ΔT_{elec} denotes the elevation in electronic temperature. The temperature dependence of the LDOS is a result of the dielectric-constant (ε) change of the material. The dielectric constant at the elevated temperature ($T_{\mathrm{elec}}+\Delta T_{\mathrm{elec}}$) was evaluated by considering the joint density of states in gold and the temperature dependence of electron distribution near the Fermi surface.[22] At the probe wavelength (λ=780 nm), the imaginary part of the dielectric constant is found to be constant, while the absolute value of the real part becomes smaller with increments of ΔT_{elec}.

The simulated transient image at the probe wavelength (780 nm) by Eq. (2) is shown in Fig. 3(b). The enhancement of the LDOS predominantly occurs at the end parts. The result explains the observed induced absorption at the ends, but does not reproduce the bleached absorption observed at the central part of the nanorod. On the other hand, if we calculate the LDOS at a longer wavelength (920 nm), where a larger contribution of the fundamental dipolar mode is expected, we obtain Fig. 3(c) as a simulated transient image. The simulated image reproduces well the observed spatial features of the transient image in Fig. 3(a). The enhancements of the LDOS at the ends arise from an increased contribution of the second LSP mode [λ_{LSP}=750 nm, corresponding to Fig. 1(b)], while the reduction of the LDOS at the center is due to a decreased contribution of the dipolar LSP mode [$\lambda_{\mathrm{LSP}}>1$ μm, Fig. 1(c)]. We believe that the simulated image at 920 nm [Fig. 3(c)] correctly reproduces the observation at 780 nm. We have a poorer agreement in the simulation at 780 nm, probably because of the DOS calculation of 780 nm in Eq. (1), which underestimates the dipolar-mode contribution relative to the second mode (discussed in the following section).

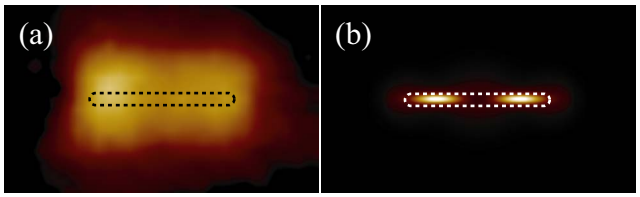

FIG. 4. (Color online) (a) Transient transmission image of a single gold nanorod (diameter 20 nm × length 240 nm) observed at 600 fs delay time. A dotted square indicates an approximate shape of the nanorod estimated from the topography measurement. Bright parts indicate regions giving bleached absorption. (b) Simulated transient transmission (LDOS change) images at 780 nm for the nanorod. Bright parts indicate regions giving a reduced LDOS.

Figure 3(d) shows DOS spectra of the gold nanorod simulated at two temperatures: at room temperature (T_{elec}=300 K) and at the elevated temperature ($T_{\mathrm{elec}}+\Delta T_{\mathrm{elec}}$=600 K). The DOS spectrum was obtained by summing the LDOS over the nanorod surface. In the calculated wavelength region, the LSP resonance peaks are redshifted at the elevated temperature due to changes in the dielectric constant. Consequently, at a wavelength in between the dipolar and the second LSP bands, the contribution of the dipolar mode (at a longer wavelength) decreases upon increases in temperature, whereas the second mode contribution increases, resulting in the $\Delta I_{\mathrm{transient}}$ image in Fig. 3(c). As recognized in the spectra in Fig. 3(d), the dipolar LSP resonance only has a minor contribution to the simulated DOS spectra at 780 nm. In contrast, in the observed spectra in Fig. 2, the dipolar mode significantly contributes at 780 nm. Judging from these facts, the simulated DOS underestimates extinction due to the dipolar mode at a wavelength of observation 780 nm. This is likely due to the fact that approximation of near-field extinction by the DOS is not valid at the tail regions of the resonance peaks. Accordingly, the LDOS contribution of the dipolar mode calculated at 920 nm is closer to the dipolar-mode contribution for the observed extinction at 780 nm. These considerations lead us to conclude that the simulated image in Fig. 3(c) appropriately reproduces the observed transient image in Fig. 3(a). This is also supported by the discussion below.

We also investigated transient images of single gold nanorods with different lengths and diameters and found that the observed spatial image contrast is strongly dependent upon the nanorod dimension. Figure 4(a) shows a transient image observed for a gold nanorod with a diameter of 20 nm and a length of 240 nm (aspect ratio=12). The transient im-

age provides an inverted contrast with respect to that observed in Fig. 3(a) (i.e., bleached absorption was found at both ends). The inversion of the image is related to the probe wavelength relative to the LSP resonance bands. For observation of the image in Fig. 3(a), the probe wavelength used was at the red side of the second LSP band (λ_{LSP}=750 nm), while that for the above-mentioned nanorod [Fig. 4(a)], with a higher aspect ratio, was at the blue side of the second LSP band (λ_{LSP}=800 nm). Since the elevation of electronic temperature induces the red shift of the LSP resonances, probing at the blue side of the LSP resonance band selectively visualizes bleached absorption and vice versa. A simulated image in Fig. 4(b) actually reproduces bleached absorptions at both ends of the nanorod, as observed in Fig. 4(a). The facts strongly support our interpretation of the transient images. We have found that transient images observed for other nanorods are also understood in a similar manner. We should note that the LDOS change arises from variation in LSP-mode wave functions due to the photoinduced transient electronic-temperature elevation in the nanorod. The present results suggest a potential for transient optical control of LSP modes by photoexcitation of metal nanostructures. This may serve as a basis for the optical control of plasmonic materials and also for a new scheme of coherent control by photoinduced dielectric-characteristic changes in the medium.

Here, we studied ultrafast dynamics of single gold nanorods using ultrafast near-field optical microscopy with a high spatial resolution. The observed transient images show characteristic spatial features that depend on the nanorod dimension studied and are ascribed to the variation of resonant LSP-mode wave functions due to the elevation in electronic temperature upon photoexcitation. The present study demonstrates that an ultrafast near-field optical method makes it possible to elucidate and manipulate dynamic, spectral, and spatial characteristics of electronic excitations in nanomaterials.

This work was supported by Grants-in-Aid for Scientific Research (Grant Nos. 18205004, 18685003, and 19049015) from the Japan Society for the Promotion of Science and from the Ministry of Education, Culture, Sports, Science and Technology.

*Author to whom correspondence should be addressed. aho@ims.ac.jp

[1] L. Novotony and B. Hecht, *Principle of Nano-optics* (Cambridge University Press, Cambridge, England, 2006).
[2] H. Okamoto and K. Imura, J. Mater. Chem. **16**, 3920 (2006).
[3] K. Imura, T. Nagahara, and H. Okamoto, J. Phys. Chem. B **108**, 16344 (2004).
[4] U. Kreibig and M. Vollmer, *Optical Properties of Metal Clusters* (Springer, Berlin, 1995).
[5] S. Kawata, *Near-field Optics and Surface Plasmon Polaritons* (Springer, Berlin, 2001).
[6] W. L. Banes, A. Dereux, and T. W. Ebbesen, Nature (London) **424**, 824 (2003).
[7] K. Kneipp, Y. Wang, H. Kneipp, L. T. Perelman, I. Itzkan, R. R. Dasari, and M. S. Feld, Phys. Rev. Lett. **78**, 1667 (1997).
[8] J. R. Lakowicz, Anal. Biochem. **337**, 171 (2005).
[9] K. Imura, H. Okamoto, M. K. Hossain, and M. Kitajima, Nano Lett. **6**, 2173 (2006).
[10] E. Ozbay, Science **311**, 189 (2006).
[11] N. Fang, H. Lee, C. Sun, and X. Zhang, Science **308**, 534 (2005).
[12] S. A. Maier and H. A. Atwater, J. Appl. Phys. **98**, 011101 (2005).
[13] S. Link and M. A. El-Sayed, J. Phys. Chem. B **103**, 8410 (1999).
[14] K. Imura, T. Nagahara, and H. Okamoto, J. Chem. Phys. **122**, 154701 (2005).
[15] C. Sönnichen, T. Franzl, T. Wilk, G. von Plessen, and J. Feldmann, Phys. Rev. Lett. **88**, 077402 (2002).
[16] A. Bouhelier, R. Bachelot, G. Lerondel, P. Royer, and G. P. Wiederrecht, Phys. Rev. Lett. **95**, 267405 (2006).
[17] M. Pelton, M. Liu, S. Park, N. F. Scherer, and P. Guyot-Sionnest, Phys. Rev. B **73**, 155419 (2006).
[18] O. L. Muskens, N. Del Fatti, and F. Vallée, Nano Lett. **6**, 552 (2006).
[19] B. D. Busbee, S. O. Obare, and C. J. Murphy, Adv. Mater. (Weinheim, Ger.) **15**, 414 (2003).
[20] C. Girard, Rep. Prog. Phys. **68**, 1883 (2005).
[21] S. D. Brorson, J. G. Fujimoto, and E. P. Ippen, Phys. Rev. Lett. **59**, 1962 (1987).
[22] M. Guerrrisi, R. Rosei, and P Winsemius, Phys. Rev. B **12**, 557 (1975).